The self-annealing phenomenon of electrodeposited nano-twin copper with high defect density

Haneul Han, Chaerin Lee, Youjung Kim, Jinhyun Lee, Sanghwa Yoon* and Bongyoung Yoo*

Department of Materials Science and Chemical Engineering, Hanyang University, Ansan, South Korea

Electroplated copper was prepared under typical conditions and a high defect density to study the effect of the defects on its self-annealing phenomenon. Two conditions, grain growth and stress relaxation during self-annealing, were analyzed with electron backscattered diffraction and a high-resolution X-ray diffractometer. Abnormal grain growth was observed in both conditions; however, the grown crystal orientation differed. The direction and relative rate at which abnormal grain growth proceeds were specified through textured orientation, and the self-annealing mechanism was studied by observing the residual stress changes over time in the films using the $\sin^2 \Psi$ method.

KEYWORDS

self-annealing, electrodeposition, nanotwins, low temperature, high current density

Introduction

As Moore's law nears its physical limits, a new type of integrated circuit device with high density is needed for the Internet of things (IoT), artificial intelligence (AI), and other wearables (Knickerbocker et al., 2018). Therefore, to achieve smaller form factors, lower power, and high performance, advanced packaging technologies, such as a 3D interconnection, are promising solutions. In advanced 3D interconnection technologies, Cu-to-Cu direct bonding has received attention because of a lower interface resistance. Electroplated Cu has been mainly studied to connect the device electrically in the Cu-to-Cu bonding (McMahon et al., 2005; Beica et al., 2008; Gueguen et al., 2010; Radisic et al., 2011; Kong et al., 2012; Liu et al., 2015). (111)-oriented nano-twinned Cu for bonding has been widely investigated because of the fastest surface diffusivity and its properties (Juang et al., 2018; Chiu et al., 2021; Lu et al., 2021). In addition, nano-twinned Cu, which has a high density of nano-twin boundaries in its grain, has attracted attention with its ultrahigh strength, ductility, high electrical conductivity, and thermal stability (Lu et al., 2004; Shen et al., 2005; Chen and Lu, 2007; Saldana et al., 2011). However, the microstructure of electroplated Cu generally changes during room temperature storage, a phenomenon termed self-annealing. Therefore, preservation of the grain orientation and nano-twin structure prior to bonding are important for connecting the bonding interface at low process temperature.

Recrystallization and grain growth occur at room temperature during a self-annealing phenomenon, unlike the conventional annealing process at high temperatures between 600°C and 1000°C (Blaz et al., 1983; Huang et al., 1997; Seah et al., 1999; Hau-Riege and Thompson, 2000; Koo and Yoon, 2001; Militzer et al., 2004; Hasegawa et al., 2006; Stangl et al., 2008). The drastic change in electrical, mechanical, and crystallographic properties was accompanied by a self-annealing phenomenon (Ritzdorf et al., 1998; Brongersma et al., 1999; Ueno et al., 1999; Lagrange et al., 2000; Hara et al., 2003; Dong et al., 2008; Cheng et al., 2010; Huang et al., 2010).

Ho et al. conducted an *in situ* investigation of the self-annealing behavior of electroplated copper films with organic additives. Copper self-annealing was accelerated by increasing the current density, and grain growth was accompanied by an increase in the twin structure and a decrease in the grain orientation spread (Ho et al., 2016). In addition, Sung et al. proposed that the defect energy causes the recrystallization of the copper film, and it can be varied depending on the deposition type, which differs by the dynamic interaction of bis-(3-sulfopropyl) disulfide (SPS) and polyethylene glycol (PEG) during electrodeposition (Sung et al., 2017). Although many papers focused on the self-annealing behavior of Cu with electrodeposition and other methods, studies about the relationships between defects, especially nano-twin lamellae, and self-annealing behaviors have not been clearly represented.

In this paper, Cu with a high density of defects and nano-twin lamellae was electroplated based on our previous research. A lower electrochemical bath temperature and higher current density generated a high density of defects with nano-twin lamellae in the Cu (Lee et al., 2020; Han et al., 2021). Crystallographic defects are formed in every material to thermodynamically stabilize the system. The defects particularly affect the intrinsic properties of materials such as the mechanical properties (Lubomirsky, 2006; du Plessis et al., 2020; Liu et al., 2020). Especially for nano-twinned Cu, one of the defects has attracted great attention because of its mechanical and electrical properties (Lu et al., 2004; Shen et al., 2005; Chen and Lu, 2007; Saldana et al., 2011). This study compared the microstructure change over time with a typical self-annealing sample, room temperature Cu (RT Cu), and a nano-twinned Cu (NT-Cu) to investigate the effect of the defects on the self-annealing phenomenon. Specifically, the effect of defects in pure Cu electroplated without any additives on the self-annealing behavior was studied by monitoring the microstructural change over time. Electron backscattered diffraction (EBSD), a high-resolution X-ray diffractometer (HR-XRD), and residual stress analysis with X-ray diffraction (XRD) were used for various microstructural analyses. Residual stress analysis in the Cu film on the substrate was characterized by XRD according to the $\sin^2\Psi$ method in which the theta angle was monitored with a variety of tilt angles (Bobet et al., 1995; Luo and Yang, 2017; Lin et al., 2020).

Experimental

Electrodeposition of Cu was conducted in a jacketed beaker (inner diameter: 10 cm; outer diameter: 14 cm; height: 20 cm) filled with an electrolyte. The Cu layer was electrodeposited on a p-type heavily doped (100) Si substrate (<0.01 Ωcm) and 200 nm Cu/20 nm Ti seed layer, which were deposited with an electron beam (e-beam) evaporation system. The two-electrode experiment was conducted with a Pt-coated mesh (7×36 mm^2) as a counter electrode and the Si wafer with a Ti and Cu seed layer covered with silicone masking tape to expose the specific area (10×10 mm^2) as the working electrode.

Cu electrodeposition was performed with a pH 1.0 acidic electrolyte adjusted with 95% sulfuric acid (0.19 M), in which the solution comprised copper sulfate (1 M) without additives was in deionized water (resistivity: 18.6 MΩ). Two types of Cu films were prepared with a programmable DC power supply (Dawoo nanotech, DADP-20010R) and a thermostatic circulator (JEIO tech, RW-0525G) to control the electrolyte temperature.
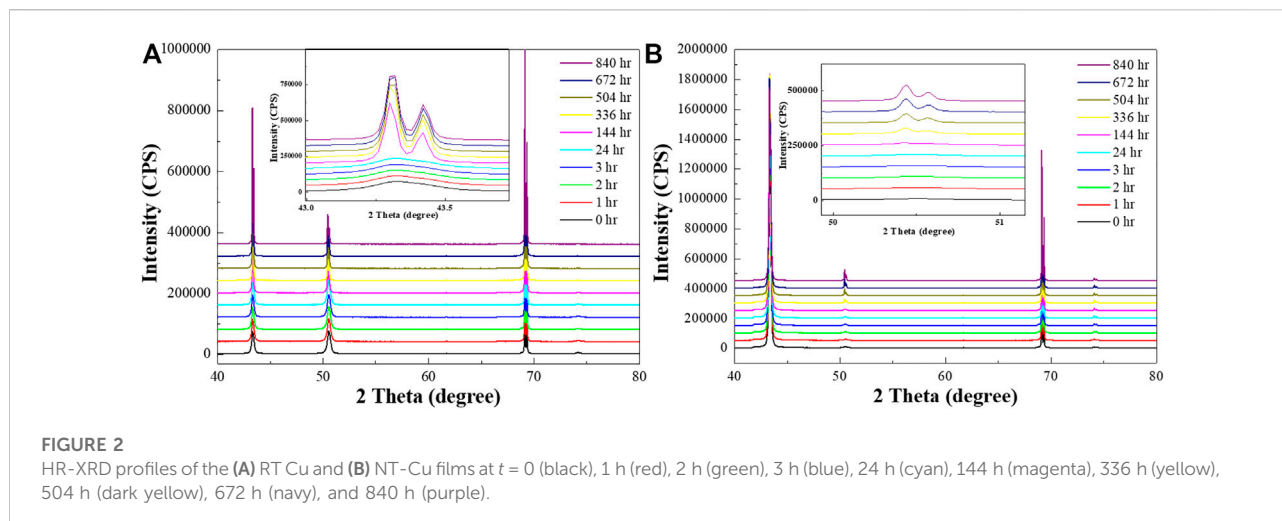
Two types of Cu specimens were prepared with different electrolyte temperature, and the same solution and plating conditions. A high current density, 210 mA/cm^2, was applied to the specimens to achieve self-annealing, which was accelerated by increasing the current density (Ho et al., 2016). However, the electrolyte temperature remained different, one was deposited at room temperature, 22.5°C, and the other at 0°C. The rotating speed was maintained at 500 rpm with an impeller coated with a stop-off lacquer to prevent other unnecessary reactions.

Crystallographic evolution during self-annealing was analyzed with EBSD operated at 20 kV, which was performed with field emission gun scanning electron microscope (FEG-SEM, 7100F, JEOL, Japan) combined with a TEAM™ PEGASUS EBSD system (EDAX, USA). The grain and grain boundary analysis were characterized with OIM™ software (EDAX). An electropolishing process was conducted for EBSD and residual stress analysis to flatten the surface of the electroplated Cu with 85% phosphoric acid. Electropolishing of Cu was applied at 4 C with a potentiostat/galvanostat (Versa STAT 4, Princeton Applied Research, USA) at room temperature.

HR-XRD (SmartLab, Rigaku, Japan) was used to characterize the preferred grain orientation of the Cu and operated at 40 kV and 30 mA from 35° to 75°. To analyze the residual stress, XRD (PANalytical; Expert pro-MPD, Almelo, Netherlands) was operated with a Cu-Kα (λ = 0.15418 nm) source generated at 40 kV and 40 mA (spot size = 3×3 mm^2). A $\sin^2\Psi$ method was analyzed in the (111) grain orientation over time with X'Pert Stress software (Baczmanski et al., 2002; Delbergue et al., 2016; Luo and Yang, 2017).
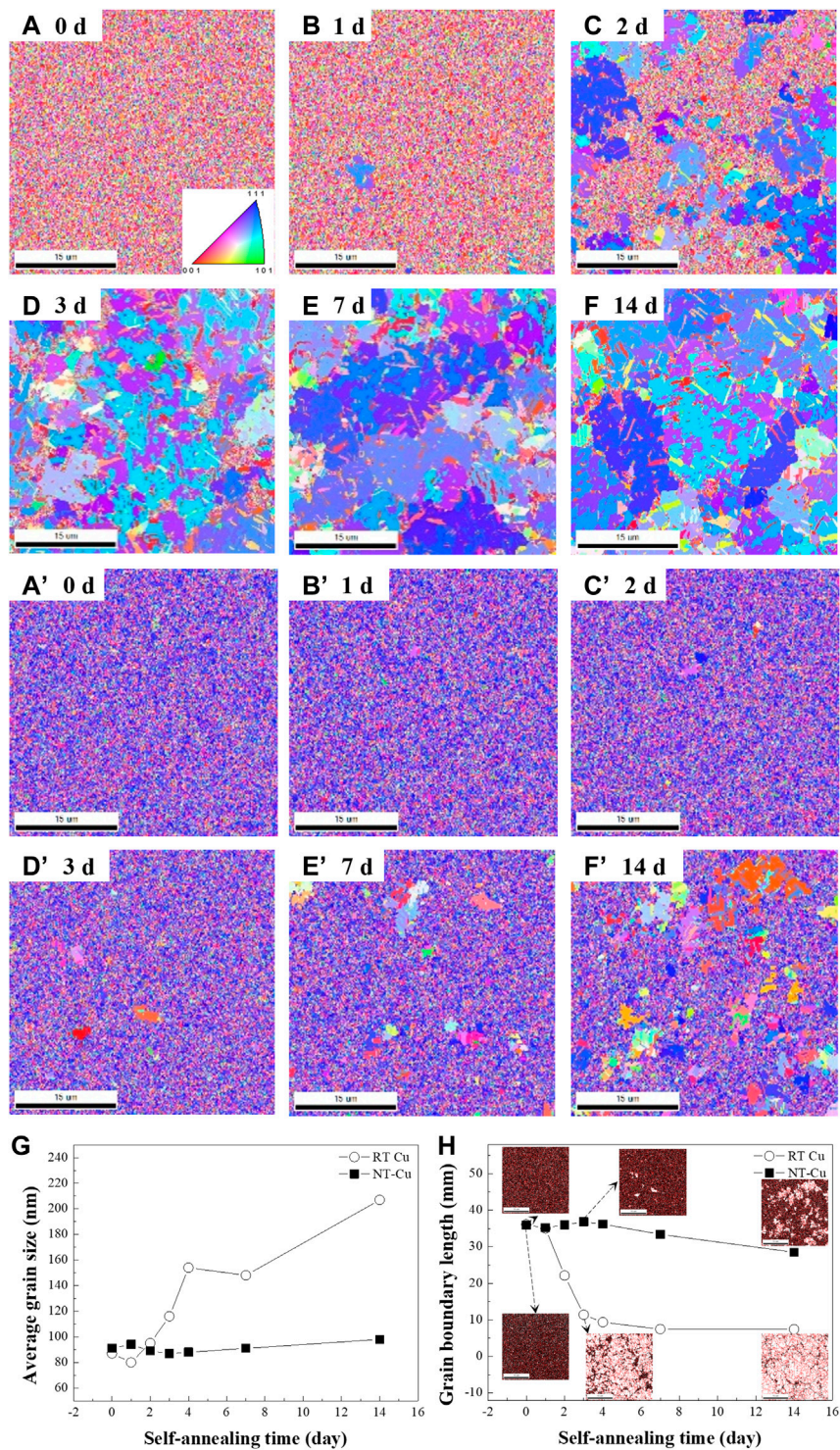
FIGURE 1
(A–F) EBSD inversed pole figures (IPFs) of the RT Cu plating at **(A)** 0, **(B)** 1, **(C)** 2, **(D)** 3, **(E)** 7, and **(F)** 14 days. **(A'–F')** IPFs of NT-Cu at the same time as **(A–F)**. **(G)** Average grain size and **(H)** grain boundary length evolution with time for RT Cu and NT-Cu.

FIGURE 2
HR-XRD profiles of the **(A)** RT Cu and **(B)** NT-Cu films at *t* = 0 (black), 1 h (red), 2 h (green), 3 h (blue), 24 h (cyan), 144 h (magenta), 336 h (yellow), 504 h (dark yellow), 672 h (navy), and 840 h (purple).

A cross-sectional image was observed by a focused ion beam (FIB, LYRA 3 XMH, TESCAN, Czech Republic). A cross-sectional sample for FIB analysis was prepared with the FIB milling performed with a small ion beam dose (current = 10 nA, voltage = 30 kV), and ion channeling contrast (current = 30 pA, voltage = 30 kV) was used to image the grains on the cross-sectional plane.

Results and discussion

Crystallographic analysis was performed over time using the EBSD and HR-XRD measurements. To verify the surface crystallographic evolution, the surface grain orientation and morphologies were characterized with EBSD analysis. The variation of the surface grains with respect to the electrolyte temperature under a current density of 210 mA/cm^2 is represented in Figures 1A–F'. Grain growth of the sample electroplated at 22.5°C (RT Cu) occurred, and the overall grain orientations changed within a week, as shown in Figures 1A–F. Alternatively, Cu electroplated at 0°C (NT-Cu) experienced abnormal grain growth over time, and the growth was not saturated, as shown in Figures 1A'–F'. Figures 1A–F shows that the RT Cu grains with random orientation grew to the (111) orientation over time, and Figures 1A'–F' shows the change of the NT-Cu grains that grew from the (111) preferred orientation to other orientations. As shown in Figures 1A–F', abnormal grain growth occurred in both specimens regardless of the condition.

HR-XRD analysis was used to study the grain orientation and texture change tendency with both conditions of Cu by time (Figure 2). Three major peaks in Cu were measured in Figure 2, corresponding with the Cu peak in PDF #03-065-9026. Figure 2A shows an increase in the (111) grain orientation peak in RT Cu, especially after one week. However, there is no drastic change in the peaks over time in NT-Cu (Figure 2B); the (200) peak appeared gradually.

To elucidate the texture changes of the specimens, the texture coefficient (TC) was calculated by Eq. 1, which was measured by HR-XRD analysis (Dixit et al., 2007; Hamid and Aal, 2009).
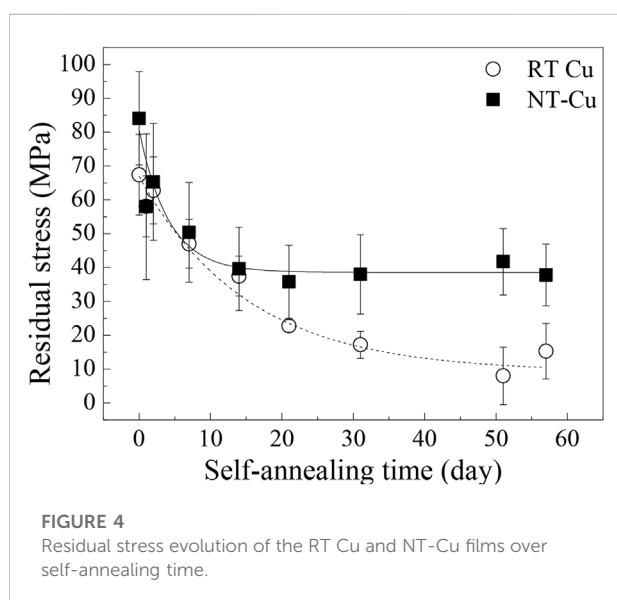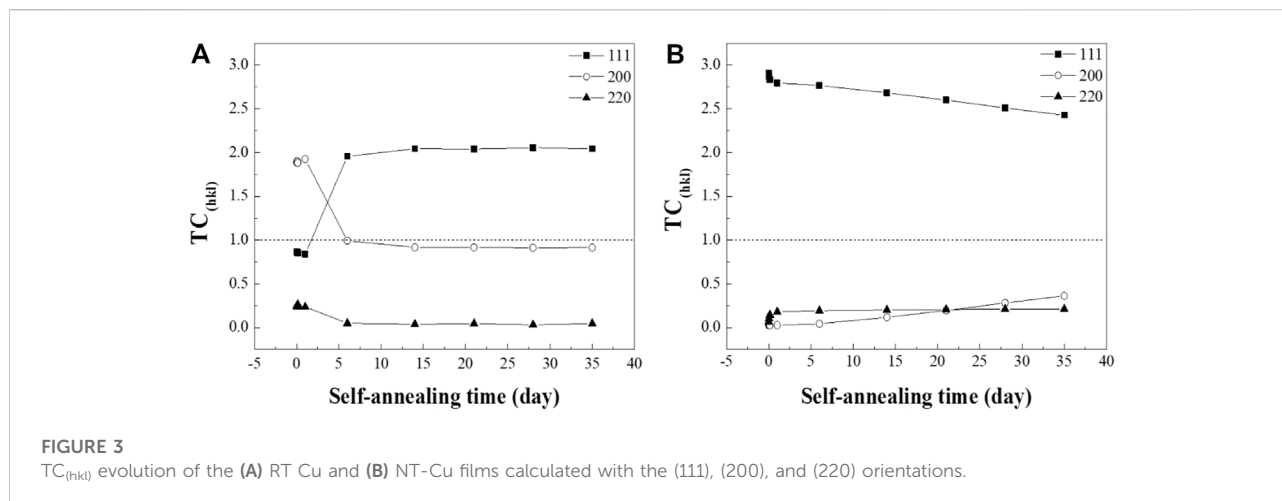
$$TC\,(hkl) = \frac{I\,(hkl)}{I_0\,(hkl)} \Big/ \frac{1}{n} \sum \frac{I\,(hkl)}{I_0\,(hkl)} \qquad (1)$$

where I(hkl) is the intensity of the samples in the experiment, I$_o$(hkl) is the standard relative intensity of the peak from PDF #03-065-9026, and n is the total number of peaks analyzed. Three prominent peaks of Cu, the (111), (200), and (220) orientations were applied to calculate the TC values. TC > 1 refers to the preferred orientation of the materials (Figure 3).

The (200) orientation of the RT Cu was dominant in the initial stage of the self-annealing, while RT Cu had the random orientation depicted in Figure 3A. Interestingly, a drastic transition from the (200) to (111) orientation was observed in the RT Cu within a week. Alternatively, the crystallographic evolution of NT-Cu was observed slowly over a long period (Figure 3B). The (111) oriented grains were illustrated as the preferred orientation of the NT-Cu during self-annealing. However, the (111) peak decreased over time while the (200) peak increased. In other words, abnormal grain growth of NT-Cu progressed with the grains in the (200) planes, while that of the RT Cu progressed with the grains in the (111) planes.

As shown in Figure 1G, both as-deposited RT Cu and NT-Cu had nanocrystalline grains with an average grain size of 87 nm and 91 nm. A high free energy per unit volume of the grain was formed because of the increase in the grain boundary area (Park et al., 2017). Grains of both RT Cu and NT-Cu were driven to grow at room temperature to reduce their internal energy because of their high grain boundary energy (Yang et al., 2019).

In the case of RT Cu, grains relatively superior to the (200) orientation in the initial stage of self-annealing changed into the (111) orientation to release the initial high internal energy. Grains with (111) planes parallel to the plane of the film have

FIGURE 3
TC$_{(hkl)}$ evolution of the **(A)** RT Cu and **(B)** NT-Cu films calculated with the (111), (200), and (220) orientations.

FIGURE 4
Residual stress evolution of the RT Cu and NT-Cu films over self-annealing time.

the lowest surface energy in the face-centered cubic (FCC) structure, which results in grain growth in a direction (Foiles et al., 1986; Udler and Seidman, 1996; Jian-Min et al., 2004; Wen and Zhang, 2007; Fishman et al., 2013). Additionally, (111) planes are conventionally known as the plane with the fastest growth rate (Thompson, 1990; Lee et al., 2001), which causes grains in RT Cu to grow rapidly in the (111) orientation. However, grains in NT-Cu grew into the (200) orientation, with the minimum strain energy in the FCC metals (Zielinski et al., 1995; Lee, 2000; Zhang et al., 2002; Zhang et al., 2005). Although the initial average grain size generated a similar grain boundary energy in both Cu, a strain energy relaxation mechanism occurred in NT-Cu. As confirmed in the previous research, NT-Cu has a high density of defects on its surface even

though it has a high density of nano-twin lamellae in its vertical grains. The defects increase the internal strain energy, causing grain growth in the direction of less strain energy (Lee et al., 2020; Han et al., 2021).

The sin$^2\Psi$ method by X-ray diffraction (XRD) was used to verify the residual stress of RT Cu and NT-Cu in the unidirectional direction over time, as shown in Figure 4. By detecting the theta value (?) according to the psi value (Ψ), residual stress in the sample was calculated by elastic modulus and Poisson's ratio of bulk Cu (Baczmanski et al., 2002; Delbergue et al., 2016; Luo and Yang, 2017).

Figure 4 shows the residual stress changes in RT Cu and NT-Cu during self-annealing. The stress in the RT Cu was calculated as 67.4 MPa in the initial stage of self-annealing and gradually decreased to approximately 8.0 MPa after 51 days. In its initial state, NT-Cu has a relatively higher stress than RT Cu (84.1 MPa), and it rapidly reduced and saturated to approximately 40 MPa, approximately 47% of the initial stress. Stress changes during self-annealing have been conventionally expressed as a stress evolution of Cu, divided into two categories: stress generation because of grain growth and stress relaxation by dislocation plasticity (Brongersma et al., 1999; Harper et al., 1999; Huang et al., 2010). Figure 4 shows that high residual stress existed in both conditions as compared to other references where it existed at the initial stage of the self-annealing (Brongersma et al., 1999; Lagrange et al., 2000).

Both conditions had a similar average grain size and grain boundary length in the initial state shown in Figures 1G,H; however, the initial stress of the two conditions differed by approximately 16.7 MPa. Internal strain generated by defects can cause stress in the metal (Dieter and Bacon, 1976). The initial internal strain caused by the grain boundary was similar, so it is expected that the initial defect density difference between the two conditions generated the residual stress difference (Basu et al.,
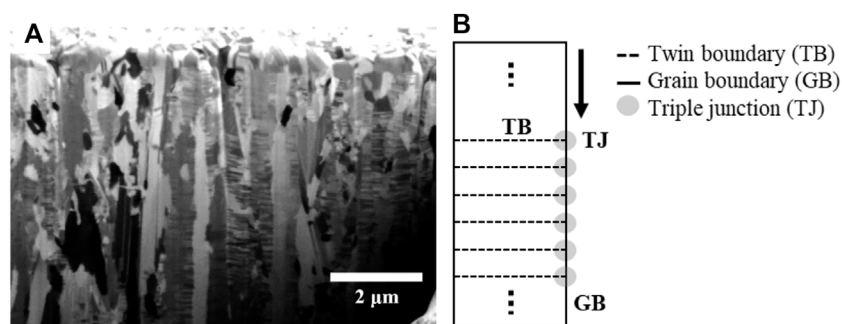
FIGURE 5
(A) Cross-sectional FIB image of as-deposited NT-Cu and **(B)** schematics of the nano-twin column with nano-twin lamellae, grain boundary, and triple junctions.

2017). Stress saturation in the NT-Cu can be supposed that the stress reached the self-diffusion equilibrium because of its defects, while RT Cu lost most of its stress and only remained approximately 10 MPa after self-annealing (Figure 4). The self-diffusion of RT Cu occurred actively over time.

Chen et al. investigated the effect of triple junctions generated with a grain boundary and twin boundary on atomic diffusion (Chen et al., 2008). The twin boundary separates the grain into two sub-grains and generates the triple junction with the grain boundary. In their research, the atomic diffusion was delayed in the triple junction between the grain boundary and twin boundary.

Figure 5A shows the high density of the nano-twin lamellae in columnar grains of the as-deposited NT-Cu. In this study, NT-Cu has a high density of nano-twin lamellae, resulting in many triple junctions between the grain boundary and twin boundary, similar to Figure 5B. The grain growth phenomenon occurs *via* atomic diffusion. Atoms mainly diffuse along the intergranular path, called grain boundary diffusion (Nieh and Nix, 1980; Kolobov et al., 2001). Therefore, self-diffusion *via* the grain boundary can be illustrated as shown in Figure 5B. It was expected that atoms diffused along the grain boundary and met the innumerable triple junctions that disturbed the diffusion. In other words, Cu atoms were diffused at both conditions; however, numerous triple junctions in the NT-Cu delayed their motions. The grain growth rate of NT-Cu is slow because of the triple junction delay.

Conclusion

The effect of the high defect density and nano-twin lamellae on the self-annealing phenomenon was investigated by analysis of the grain morphology, orientation, texture, and residual stress. Grains of NT-Cu grew to the (200) orientation, while RT Cu grew to the (111) orientation according to EBSD and HR-XRD

analysis. Both conditions had a similar average grain size; however, their crystalline evolution patterns and rates differed. In particular, RT Cu grains grew and saturated within a week, whereas NT-Cu grains grew gradually and did not saturate after a month. However, the opposite tendency was observed in residual stress. Residual stress in RT Cu gradually decreased over time, and the stress in NT-Cu was dramatically reduced in the initial stage of self-annealing and saturated at 50%. As a result, the high defect density contributed to the grain growth texture and the nano-twin lamellae contributed to the self-diffusion rate at room temperature.

Data availability statement

The original contributions presented in the study are included in the article/Supplementary material, further inquiries can be directed to the corresponding authors.

Author contributions

The study was designed by SY and BY. The experimental work was carried out by HH, CL, and YK Data analysis was performed by JL and HH. All authors contributed to write the manuscript.

Funding

Conflict of interest

The authors declare that the research was conducted in the absence of any commercial or financial relationships that could be construed as a potential conflict of interest.

The handling editor declared a past co-authorship with the authors JL, BY, and YK.

Publisher's note

All claims expressed in this article are solely those of the authors and do not necessarily represent those of their affiliated organizations, or those of the publisher, the editors and the reviewers. Any product that may be evaluated in this article, or claim that may be made by its manufacturer, is not guaranteed or endorsed by the publisher.

References

Baczmanski, A., Lark, R. J., and Skrzypek, S. J. (2002). Application of non-linear sin^{2}ψ method for stress determination using X-ray diffraction. *Mater. Sci. Forum* 404-407, 29–34. doi:10.4028/www.scientific.net/msf.404-407.29

Basu, I., Ocelík, V., and De Hosson, J. T. M. (2017). *Experimental determination and theoretical analysis of local residual stress at grain scale*. Chilworth: WIT Press.

Beica, R., Sharbono, C., and Ritzdorf, T. (2008). ""Through silicon via copper electrodeposition for 3D integration," in 2008 58th Electronic Components and Technology Conference, 577–583.

Blaz, L., Sakai, T., and Jonas, J. J. (1983). Effect of initial grain size on dynamic recrystallization of copper. *Metal Sci.* 17 (12), 609–616. doi:10.1179/030634583790420448

Bobet, J. L., Naslain, R., Guette, A., Ji, N., and Lebrun, J. L. (1995). Thermal residual stresses in ceramic matrix composites—II. Experimental results for model materials. *Acta Metallurgica Materialia* 43 (6), 2255–2268. doi:10.1016/0956-7151(94)00430-7

Brongersma, S. H., Richard, E., Vervoort, I., Bender, H., Vandervorst, W., Lagrange, S., et al. (1999). Two-step room temperature grain growth in electroplated copper. *J. Appl. Phys.* 86 (7), 3642–3645. doi:10.1063/1.371272

Chen, K.-C., Wu, W.-W., Liao, C.-N., Chen, L.-J., and Tu, K. N. (2008). Observation of atomic diffusion at twin-modified grain boundaries in copper. *Science* 321 (5892), 1066–1069. doi:10.1126/science.1160777

Chen, X. H., and Lu, L. (2007). Work hardening of ultrafine-grained copper with nanoscale twins. *Scr. Mater.* 57 (2), 133–136. doi:10.1016/j.scriptamat.2007.03.029

Cheng, M.-Y., Chen, K.-W., Liu, T.-F., Wang, Y.-L., and Feng, H.-P. (2010). Effects of direct current and pulse-reverse copper plating waveforms on the incubation behavior of self-annealing. *Thin Solid Films* 518 (24), 7468–7474. doi:10.1016/j.tsf.2010.05.026

Chiu, W. L., Lee, O. H., Chiang, C. W., and Chang, H. H. (2021). "Low temperature wafer-to-wafer hybrid bonding by nanotwinned copper," in 2021 IEEE 71st Electronic Components and Technology Conference (ECTC)), 365–370.

Delbergue, D., Texier, D., Levesque, M., and Bocher, P. (2016). "Comparison of two X-ray residual stress measurement methods: Sin2 ψ and cos α, through the determination of a martensitic steel X-ray elastic constant," in International conference on Residual Stresses, 55–60.

Dieter, G. E., and Bacon, D. (1976). *Mechanical metallurgy*. New York: McGraw-Hill.

Dixit, P., Xu, L., Miao, J., Pang, J. H. L., and Preisser, R. (2007). Mechanical and microstructural characterization of high aspect ratio through-wafer electroplated copper interconnects. *J. Micromech. Microeng.* 17 (9), 1749–1757. doi:10.1088/0960-1317/17/9/001

Dong, W., Zhang, J., Zheng, J., and Sheng, J. (2008). Self-annealing of electrodeposited copper thin film during room temperature storage. *Mater. Lett.* 62 (10), 1589–1591. doi:10.1016/j.matlet.2007.09.029

du Plessis, A., Yadroitsava, I., and Yadroitsev, I. (2020). Effects of defects on mechanical properties in metal additive manufacturing: A review focusing on X-ray tomography insights. *Mater. Des.* 187, 108385. doi:10.1016/j.matdes.2019.108385

Fishman, M., Zhuang, H. L., Mathew, K., Dirschka, W., and Hennig, R. G. (2013). Accuracy of exchange-correlation functionals and effect of solvation on the surface energy of copper. *Phys. Rev. B* 87 (24), 245402. doi:10.1103/PhysRevB.87.245402

Foiles, S. M., Baskes, M. I., and Daw, M. S. (1986). Embedded-atom-method functions for the fcc metals Cu, Ag, Au, Ni, Pd, Pt, and their alloys. *Phys. Rev. B* 33 (12), 7983–7991. doi:10.1103/PhysRevB.33.7983

Gueguen, P., Cioccio, L. D., Morfouli, P., Zussy, M., Dechamp, J., Bally, L., et al. (2010). ""Copper direct bonding: An innovative 3D interconnect," in 2010 Proceedings 60th Electronic Components and Technology Conference, 878–883.

Hamid, Z. A., and Aal, A. A. (2009). New environmentally friendly noncyanide alkaline electrolyte for copper electroplating. *Surf. Coatings Technol.* 203 (10), 1360–1365. doi:10.1016/j.surfcoat.2008.11.001

Han, H., Lee, C., Kim, Y., Lee, J., Kim, R., Kim, J., et al. (2021). Cu to Cu direct bonding at low temperature with high density defect in electrodeposited Cu. *Appl. Surf. Sci.* 550, 149337. doi:10.1016/j.apsusc.2021.149337

Hara, T., Toida, H., and Shimura, Y. (2003). The self-annealing phenomenon in copper interconnection. *Electrochem. Solid-State Lett.* 6 (7), G98. doi:10.1149/1.1576572

Harper, J. M. E., Cabral, C., Andricacos, P. C., Gignac, L., Noyan, I. C., Rodbell, K. P., et al. (1999). Mechanisms for microstructure evolution in electroplated copper thin films near room temperature. *J. Appl. Phys.* 86 (5), 2516–2525. doi:10.1063/1.371086

Hasegawa, M., Nonaka, Y., Negishi, Y., Okinaka, Y., and Osaka, T. (2006). Enhancement of the ductility of electrodeposited copper films by room-temperature recrystallization. *J. Electrochem. Soc.* 153 (2), C117. doi:10.1149/1.2149299

Hau-Riege, S. P., and Thompson, C. V. (2000). *In situ* transmission electron microscope studies of the kinetics of abnormal grain growth in electroplated copper films. *Appl. Phys. Lett.* 76 (3), 309–311. doi:10.1063/1.125729

Ho, C.-E., Chen, C.-C., Lu, M.-K., Lee, Y.-W., and Wu, Y.-S. (2016). *In-situ* study on the self-annealing behavior of electroplated Cu through the cantilever method, XRD, and EBSD. *Surf. Coatings Technol.* 303, 86–93. doi:10.1016/j.surfcoat.2016.02.052

Huang, J. S., Zhang, J., Cuevas, A., and Tu, K. N. (1997). Recrystallization and grain growth in bulk Cu and Cu(Sn) alloy. *Mater. Chem. Phys.* 49 (1), 33–41. doi:10.1016/S0254-0584(97)80124-1

Huang, R., Robl, W., Ceric, H., Detzel, T., and Dehm, G. (2010). Stress, sheet resistance, and microstructure evolution of electroplated Cu films during self-annealing. *IEEE Trans. Device Mat. Reliab.* 10 (1), 47–54. doi:10.1109/TDMR.2009.2032768

Jian-Min, Z., Fei, M., and Ke-Wei, X. (2004). Calculation of the surface energy of fcc metals with modified embedded-atom method. *Chin. Phys.* 13 (7), 1082–1090. doi:10.1088/1009-1963/13/7/020

Juang, J.-Y., Lu, C.-L., Chen, K.-J., Chen, C.-C. A., Hsu, P.-N., Chen, C., et al. (2018). Copper-to-copper direct bonding on highly (111)-oriented nanotwinned copper in no-vacuum ambient. *Sci. Rep.* 8 (1), 13910. doi:10.1038/s41598-018-32280-x

Knickerbocker, J. U., Budd, R., Dang, B., Chen, Q., Colgan, E., Hung, L. W., et al. (2018). "Heterogeneous integration technology demonstrations for future healthcare, IoT, and AI computing solutions," in 2018 IEEE 68th Electronic Components and Technology Conference (ECTC)), 1519–1528.

Kolobov, Y. R., Grabovetskaya, G. P., Ivanov, M. B., Zhilyaev, A. P., and Valiev, R. Z. (2001). Grain boundary diffusion characteristics of nanostructured nickel. *Scr. Mater.* 44 (6), 873–878. doi:10.1016/S1359-6462(00)00699-0

Kong, L., Rudack, A. C., Krueger, P., Zschech, E., Arkalgud, S., and Diebold, A. C. (2012). 3D-interconnect: Visualization of extrusion and voids induced in copper-filled through-silicon vias (TSVs) at various temperatures using X-ray microscopy. *Microelectron. Eng.* 92, 24–28. doi:10.1016/j.mee.2011.04.012

Koo, J. B., and Yoon, D. Y. (2001). Abnormal grain growth in bulk Cu—the dependence on initial grain size and annealing temperature. *Metall. Mat. Trans. A* 32 (8), 1911–1926. doi:10.1007/s11661-001-0004-2

Lagrange, S., Brongersma, S. H., Judelewicz, M., Saerens, A., Vervoort, I., Richard, E., et al. (2000). Self-annealing characterization of electroplated copper films. *Microelectron. Eng.* 50 (1), 449–457. doi:10.1016/S0167-9317(99)00314-7

Lee, C., Kim, Y., Kim, R., Yoo, B., and Kim, J.-K. (2020). Evolution of microstructures and mechanical properties of ultrahigh strength, pure

electrodeposited Cu during self-annealing. *J. Alloys Compd.* 846, 156488. doi:10.1016/j.jallcom.2020.156488

Lee, D.-S., Park, D.-Y., Woo, H.-J., Kim, S.-H., Ha, J., and Yoon, E. (2001). Preferred orientation controlled giant grain growth of platinum thin films on SiO2/Si substrates. *Jpn. J. Appl. Phys. (2008).* 40, L1–L3. doi:10.1143/jjap.40.l1

Lee, D. N. (2000). Strain energy release maximization model for evolution of recrystallization textures. *Int. J. Mech. Sci.* 42 (8), 1645–1678. doi:10.1016/S0020-7403(99)00095-8

Lin, Q., Fan, Z., Wang, W., Yan, Z., Zheng, Q., and Mei, X. (2020). The effect of spot overlap ratio on femtosecond laser planarization processing of SiC ceramics. *Opt. Laser Technol.* 129, 106270. doi:10.1016/j.optlastec.2020.106270

Liu, C.-M., Lin, H.-W., Huang, Y.-S., Chu, Y.-C., Chen, C., Lyu, D.-R., et al. (2015). Low-temperature direct copper-to-copper bonding enabled by creep on (111) surfaces of nanotwinned Cu. *Sci. Rep.* 5 (1), 9734. doi:10.1038/srep09734

Liu, Y., Cao, Y., Mao, Q., Zhou, H., Zhao, Y., Jiang, W., et al. (2020). Critical microstructures and defects in heterostructured materials and their effects on mechanical properties. *Acta Mater.* 189, 129–144. doi:10.1016/j.actamat.2020.03.001

Lu, L., Shen, Y., Chen, X., Qian, L., and Lu, K. (2004). Ultrahigh strength and high electrical conductivity in copper. *Science* 304 (5669), 422–426. doi:10.1126/science.1092905

Lu, T.-F., Lai, T.-Y., Chu, Y. Y., and Wu, Y. S. (2021). Effect of nanotwin boundary on the Cu–Cu bonding. *ECS J. Solid State Sci. Technol.* 10 (7), 074001. doi:10.1149/2162-8777/ac0e14

Lubomirsky, I. (2006). Mechanical properties and defect chemistry. *Solid State Ionics* 177 (19), 1639–1642. doi:10.1016/j.ssi.2006.01.020

Luo, Q., and Yang, S. (2017). Uncertainty of the X-ray diffraction (XRD) sin2 ψ technique in measuring residual stresses of physical vapor deposition (PVD) hard coatings. *Coatings* 7 (8), 128. doi:10.3390/coatings7080128

McMahon, J. J., Lu, J. Q., and Gutmann, R. J. (2005). "Wafer bonding of damascene-patterned metal/adhesive redistribution layers for via-first three-dimensional (3D) interconnect," in Proceedings Electronic Components and Technology, 331–336.(

Militzer, M., Freundlich, P., and Bizzotto, D. (2004). Abnormal grain growth in electrochemically deposited Cu films. *Mater. Sci. Forum* 467-470, 1339–1344. doi:10.4028/www.scientific.net/msf.467-470.1339

Nieh, T. G., and Nix, W. D. (1980). The formation of water vapor bubbles in copper and their effect on intergranular creep fracture. *Acta Metall.* 28 (5), 557–566. doi:10.1016/0001-6160(80)90122-4

Park, M. H., Lee, Y. H., Kim, H. J., Schenk, T., Lee, W., Kim, K. D., et al. (2017). Surface and grain boundary energy as the key enabler of ferroelectricity in nanoscale hafnia-zirconia: A comparison of model and experiment. *Nanoscale* 9 (28), 9973–9986. doi:10.1039/C7NR02121F

Radisic, A., Lühn, O., Philipsen, H. G. G., El-Mekki, Z., Honore, M., Rodet, S., et al. (2011). Copper plating for 3D interconnects. *Microelectron. Eng.* 88 (5), 701–704. doi:10.1016/j.mee.2010.06.030

Ritzdorf, T., Graham, L., Jin, S., Mu, C., and Fraser, D. (1998). ""Self-annealing of electrochemically deposited copper films in advanced interconnect applications," in Proceedings of the IEEE 1998 International Interconnect Technology Conference, 166–168.

Saldana, C., King, A. H., Stach, E. A., Compton, W. D., and Chandrasekar, S. (2011). Vacancies, twins, and the thermal stability of ultrafine-grained copper. *Appl. Phys. Lett.* 99 (23), 231911. doi:10.1063/1.3669404

Seah, C. H., Mridha, S., and Chan, L. H. (1999). Annealing of copper electrodeposits. *J. Vac. Sci. Technol. A Vac. Surfaces Films* 17 (4), 1963–1967. doi:10.1116/1.581711

Shen, Y. F., Lu, L., Lu, Q. H., Jin, Z. H., and Lu, K. (2005). Tensile properties of copper with nano-scale twins. *Scr. Mater.* 52 (10), 989–994. doi:10.1016/j.scriptamat.2005.01.033

Stangl, M., Lipták, M., Fletcher, A., Acker, J., Thomas, J., Wendrock, H., et al. (2008). Influence of initial microstructure and impurities on Cu room-temperature recrystallization (self-annealing). *Microelectron. Eng.* 85 (3), 534–541. doi:10.1016/j.mee.2007.09.007

Sung, M., Kim, H. C., Lim, T., and Kim, J. J. (2017). Effects of organic additives on grain growth in electrodeposited Cu thin film during self-annealing. *J. Electrochem. Soc.* 164 (13), D805–D809. doi:10.1149/2.0481713jes

Thompson, C. V. (1990). Grain growth in thin films. *Annu. Rev. Mat. Sci.* 20 (1), 245–268. doi:10.1146/annurev.ms.20.080190.001333

Udler, D., and Seidman, D. N. (1996). Grain boundary and surface energies of fcc metals. *Phys. Rev. B* 54 (16), R11133–R11136. doi:10.1103/PhysRevB.54.R11133

Ueno, K., Ritzdorf, T., and Grace, S. (1999). Seed layer dependence of room-temperature recrystallization in electroplated copper films. *J. Appl. Phys.* 86 (9), 4930–4935. doi:10.1063/1.371462

Wen, Y.-N., and Zhang, J.-M. (2007). Surface energy calculation of the fcc metals by using the MAEAM. *Solid State Commun.* 144 (3), 163–167. doi:10.1016/j.ssc.2007.07.012

Yang, C.-H., Lee, Y.-W., Lee, C.-Y., Chang, C.-H., and Ho, C.-E. (2019). Self-annealing behavior of electroplated Cu in blind-hole structures. *J. Electrochem. Soc.* 166 (13), D683–D688. doi:10.1149/2.1301913jes

Zhang, J.-M., Xu, K.-W., and Ji, V. (2002). Dependence of strain energy on the grain orientations in an FCC-polycrystalline film on rigid substrate. *Appl. Surf. Sci.* 185 (3), 177–182. doi:10.1016/S0169-4332(01)00586-4

Zhang, J.-M., Zhang, Y., and Xu, K.-W. (2005). Dependence of stresses and strain energies on grain orientations in FCC metal films. *J. Cryst. Growth* 285 (3), 427–435. doi:10.1016/j.jcrysgro.2005.08.037

Zielinski, E. M., Vinci, R. P., and Bravman, J. C. (1995). The influence of strain energy minimization on abnormal grain growth in copper thin films. *MRS Proc.* 391, 103. doi:10.1557/PROC-391-103